

Supporting Information:

**Contrast-variation Time-resolved SANS Analysis of Oil Exchange
Kinetics Between Oil-in-water Emulsions Stabilized by Anionic
Surfactants**

Yi-Ting Lee¹ and Lilo D. Pozzo^{1}*

1: Department of Chemical Engineering, University of Washington, Seattle, WA, USA

*E-mail: dpozzo@uw.edu

*Phone: 1-206-685-8536

Tables of contents:

Pages S1-28

Figure S1-30

Table S1-S3

Emulsion contrast matching point optimization

The overall measured scattering intensity is correlated with the sample transmission (T) and contrast ($\Delta\rho$) as shown in equation S1. Moreover, the contrast of the two stock emulsion systems can be expressed as equation S2, where $SLD_{emulsion1}$ and $SLD_{emulsion2}$ are scattering length densities (SLD) of the two populations of emulsions that are consistent of hydrogenated/deuterated hexadecane and $SLD_{solvent}$ is the scattering length density of the solvent (H_2O and D_2O mixture). Ideally one would choose to use a fully deuterated hexadecane as the high SLD emulsion ($SLD = 6.66 \times 10^{-6} \text{ \AA}^{-2}$) and fully hydrogenated hexadecane as the low SLD emulsion ($SLD = -0.43 \times 10^{-6} \text{ \AA}^{-2}$) as the two initial emulsion stocks. Based on this emulsion composition, the corresponding SLD of the solvent could then be estimated to be $3.11 \times 10^{-6} \text{ \AA}^{-2}$, which consists of 46 vol% H_2O and 54 vol% D_2O . However, if oil exchange experiments were performed using this contrast matching condition and a long pathlength sample cell (i.e. 1 cm), the large absorption cross-section of H_2O in the solvent would absorb nearly all of the neutrons passing through the system and minimal scattering intensities would be detected (transmission $\sim 3\%$). Thus, a balance between the emulsion contrast and sample transmission must be considered to optimize contrast matching of the emulsion systems.

$$I \propto T \cdot \Delta\rho^2 \quad (S1)$$

$$\Delta\rho^2 = (SLD_{Emulsion1} - SLD_{solvent})^2 = (SLD_{solvent} - SLD_{Emulsion2})^2 \quad (S2)$$

The first step for estimating the optimized contrast matching condition is to simplify equation S2 to minimize the number of parameters used in the calculation. The equation can be re-organized to express the fully exchanged system that is contrast matched. In addition, the amount

of deuterated hexadecane (D-hexadecane) and hydrogenated hexadecane (H-hexadecane) in this system can be expressed in its corresponding volume fraction. For example, the fully mixed emulsion contains X_{hex} H-hexadecane and $X_{\text{D-hex}}$ D-hexadecane, which can also be expressed as $(1 - X_{\text{hex}})$. The same process can also be performed to the solvent such that the mixture is expressed only using the volume fraction of H_2O (equation S3). The SLD values of the different components are constants that can be estimated using the NIST neutron activation and scattering calculator. Thus, the emulsion contrast matching condition can be simplified to using only one parameter (either in X_{hex} or $X_{\text{H}_2\text{O}}$) as shown in equation S4.

$$\begin{aligned} X_{\text{hex}} * \text{SLD}_{\text{hex}} + (1 - X_{\text{hex}}) * \text{SLD}_{\text{D-hex}} \\ = X_{\text{H}_2\text{O}} * \text{SLD}_{\text{H}_2\text{O}} + (1 - X_{\text{H}_2\text{O}}) * \text{SLD}_{\text{D}_2\text{O}} \end{aligned} \quad (\text{S3})$$

$$X_{\text{H}_2\text{O}} = 1.022X_{\text{Hex}} - 0.0417 \quad (\text{S4})$$

The other part of the optimization process is to account for the sample transmission (T) that decays exponentially. It can be expressed using Equation S5, where d is the sample pathlength and Λ is total cross section of the solvent. The value of the total cross section can be estimated using a linear combination of the cross sections of H_2O (6.93 cm^{-1} for a 6\AA source) and D_2O (0.72 cm^{-1}). For example, a solvent containing 25% H_2O and 75% D_2O results in a total solvent cross section of 2.27 cm^{-1} .

$$T = e^{-d/\Lambda} \quad (\text{S5})$$

The measured scattering intensity can then be estimated using equation S1 and the estimated result is shown in Figure S1. As can be seen in the figure, the optimal sample configuration should contain a contrast matched oil that consists of 30% H-hexadecane and 70%

D-hexadecane. The corresponding solvent mixture would contain roughly 26.5% H₂O and 73.5% D₂O, which would provide 9% neutron transmission through a 1 cm pathlength sample.

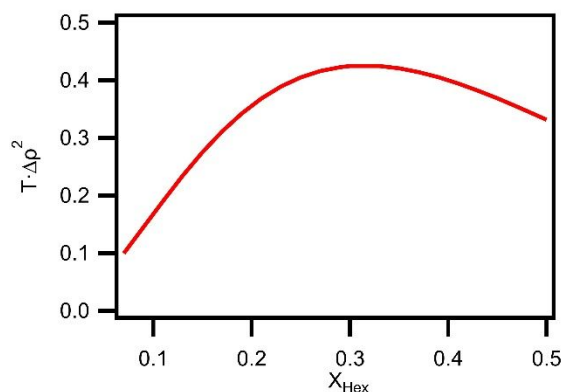


Figure S1. Hexadecane emulsion contrast matching optimization.

Contrast matching point validation

While the contrast matching configuration for the emulsion system could be estimated using the equations above, using the estimated values of the hydrogenated/deuterated material to make the sample could result in synthesizing a system that is not perfectly contrast matched. The mismatch between the calculation and the experimental measurement is due to variations in the quality of raw materials that are purchased. The purity of the components affects the actual scattering length of the samples. Therefore, the estimated SLD of the different materials may not be entirely identical to the theoretically estimated value. Thus, it is crucial to validate that the synthesized system is actually contrast-matched before conducting any time-resolved contrast variation SANS experiments.

The experimental contrast matching condition can be obtained by synthesizing the theoretically estimated contrast matching oil mixture (30% H-hexadecane and 70% D-hexadecane) in solvents with various amounts of H₂O/D₂O. The scattering profiles for each sample can be collected and the actual contrast matching point would be the condition where minimal scattering is observed. An alternative method for estimating the contrast matching point is to plot out the

square root of the scattering intensity at a specific q versus the volume fraction of D_2O in the solvent. The obtained result should resemble a ‘V’ shape since any contrast mismatch in the emulsion system would result in a higher observed scattering intensity.

The curve can be further modified such that the contrast matching condition could be mathematically estimated. In short, the curve was linearized by multiplying half of the ‘V’ data point values by -1 as shown in Figure S2. The contrast matching point of the system would be the condition in which the line crosses the x-axis. For our system, the actual experimental contrast matching point occurred when the solvent contained 73.1% D_2O and 26.9% H_2O , which is relatively close to the theoretical calculation of 73.5% D_2O and 26.5% H_2O . Additional contrast matching validation experiments were also conducted for dodecane and octane systems.

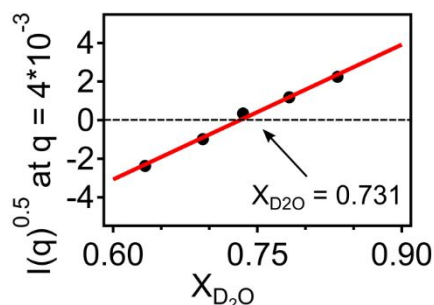


Figure S2. Hexadecane contrast matching evaluation

Quantification of structure factors on CV-SANS of dilute emulsions

The effects of the presence of a structure factor to the recorded scattering intensity was modeled using SASView. Modeled scattering intensities for a system containing 1 and 10 vol% of 60 nm radius spheres (0.1 PDI) with and without the presence of a structure factor (either hard-sphere or Hayter-Pendfold MSA) are shown in Figure S3. As can be seen in the figure, scattering intensities for a dilute system is not affected by the presence of a structure factor (hard-sphere or Hayter-Pendfold MSA).

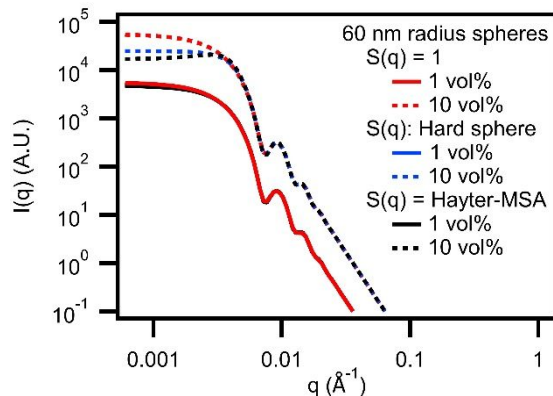


Figure S3. Theoretical model of 1 and 10 vol% of 60 nm radius spheres with and without the presence of structure factors (hard-sphere or Hayter-Pendfold MSA).

Scattering profiles of high SLD and low SLD emulsion control samples

Scattering profiles of high and low SLD control emulsions stabilized by either 1 or 20 mM of SDS were obtained as shown in Figure S4 (a). As can be seen in the figure, all of the scattering profiles overlap, suggesting that our contrast matching calculations and experimental preparation methods are adequate. Moreover, scattering profiles of different high SLD emulsion sample were also recorded at various temperatures as shown in Figure S4 (b). The scattering profiles also overlaps, suggesting our emulsion synthesis method was reliable and would result in synthesizing the same sized droplets.

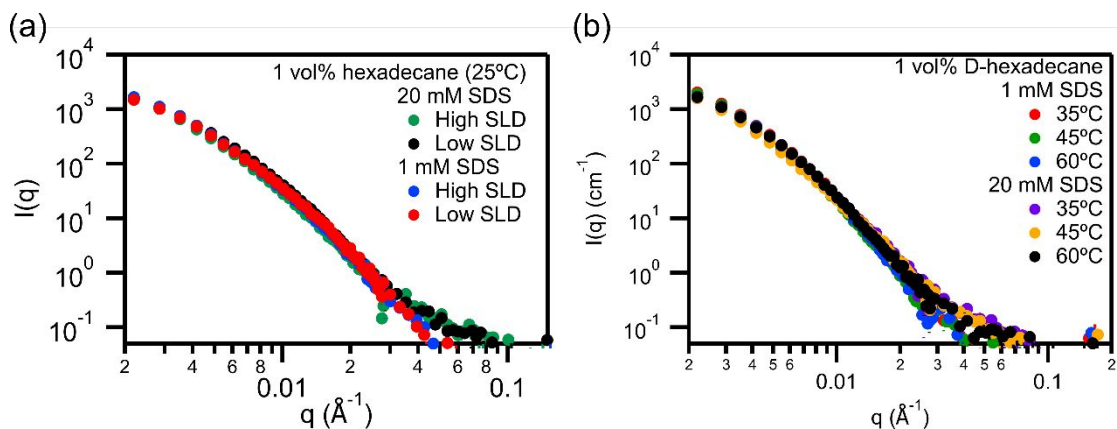


Figure S4. (a) Overlapping high SLD (100% D-hexadecane) and low SLD (40% D-hexadecane and 60% H-hexadecane) control emulsion samples stabilized by 1 and 20 mM SDS. (b) Overlapping high SLD emulsions stabilized by 1 and 20 mM SDS at various temperatures.

Estimated droplet size distribution of sonicated samples using recorded scattering profiles fitted with a polydisperse sphere model

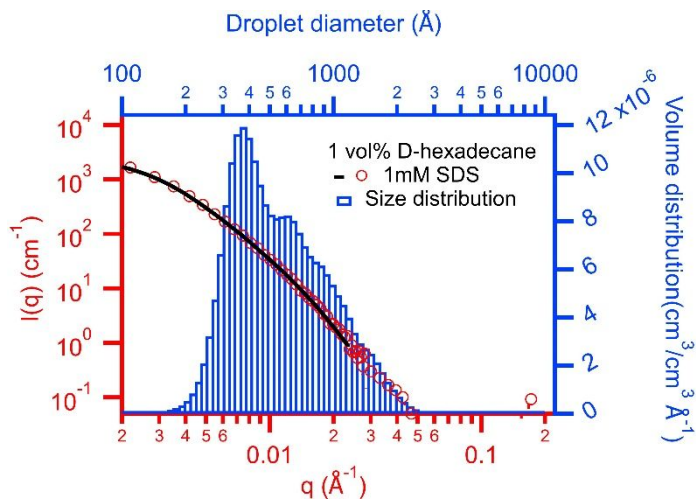


Figure S5. Example droplet size distribution (100% D-hexadecane stabilized by 1 mM SDS) obtained from fitting the recorded scattering profile with a polydisperse sphere model using Irena.¹

Scattering profiles and modeled fits of emulsion oil exchange at various surfactant concentrations, salt concentrations, and temperatures

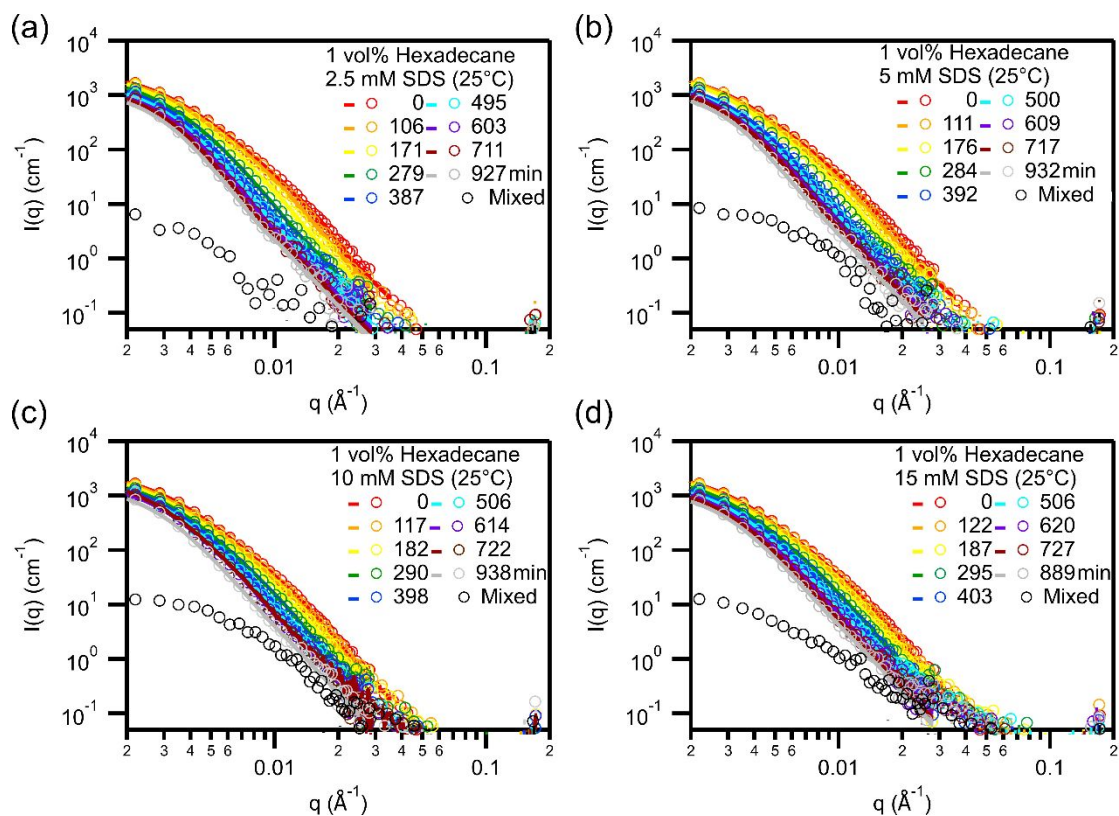


Figure S6. Oil exchange between hexadecane droplets stabilized by (a) 2.5, (b) 5, (c) 10, and (d) 15 mM sodium dodecyl sulfate (SDS) (25 °C). The rate of decay in scattering intensities is similar across various stabilizing surfactant concentrations. Lines represent fits to a polydisperse sphere model (Eq. 1 and 2 in manuscript).

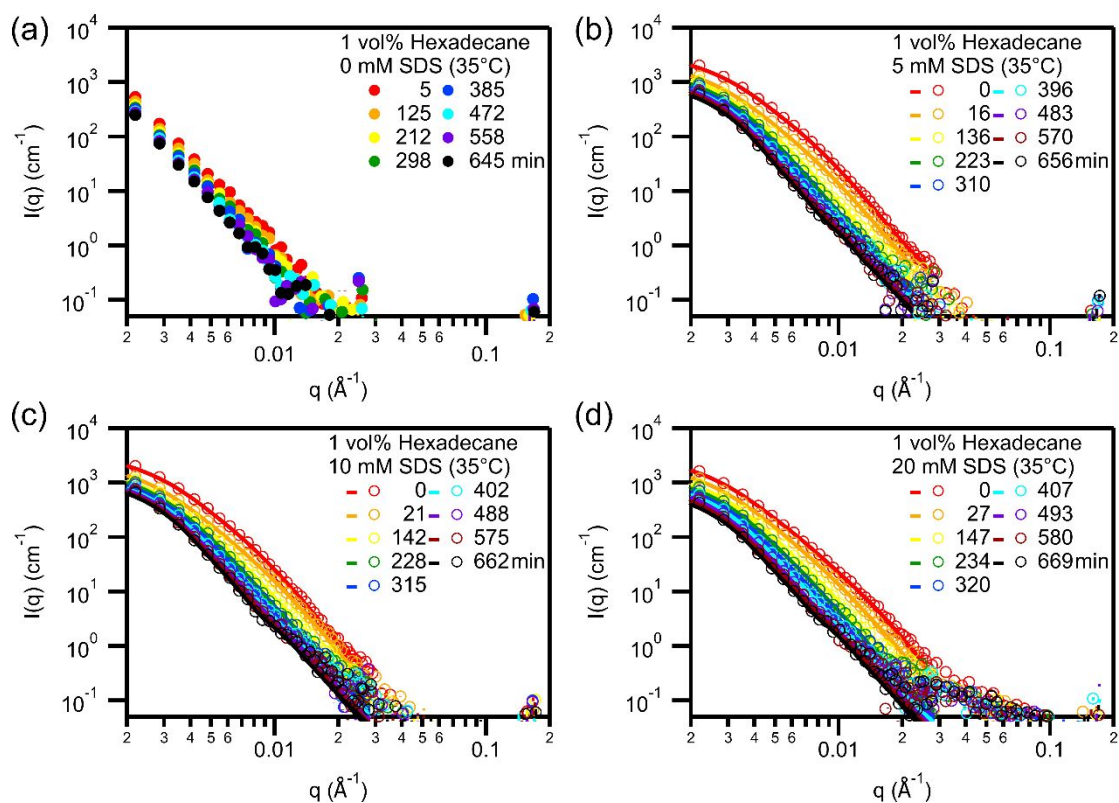


Figure S7. Oil exchange between hexadecane droplets with the presence of (a) 0, (b) 5, (c) 10, and (d) 20 mM SDS (35 °C). Lines represent fits to a polydisperse sphere model (Eq. 1 and 2 in manuscript).

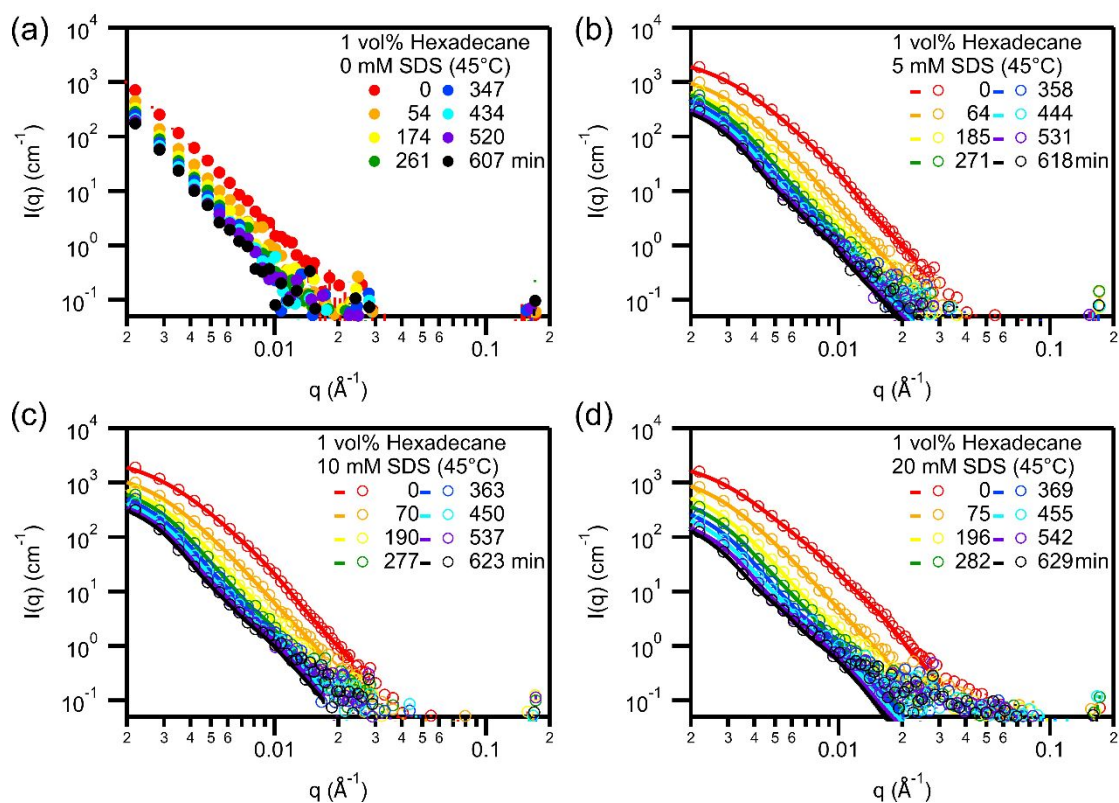


Figure S8. Oil exchange between hexadecane droplets with the presence of (a) 0, (b) 5, (c) 10, and (d) 20 mM SDS (45 °C). Lines represent fits to a polydisperse sphere model (Eq. 1 and 2 in manuscript).

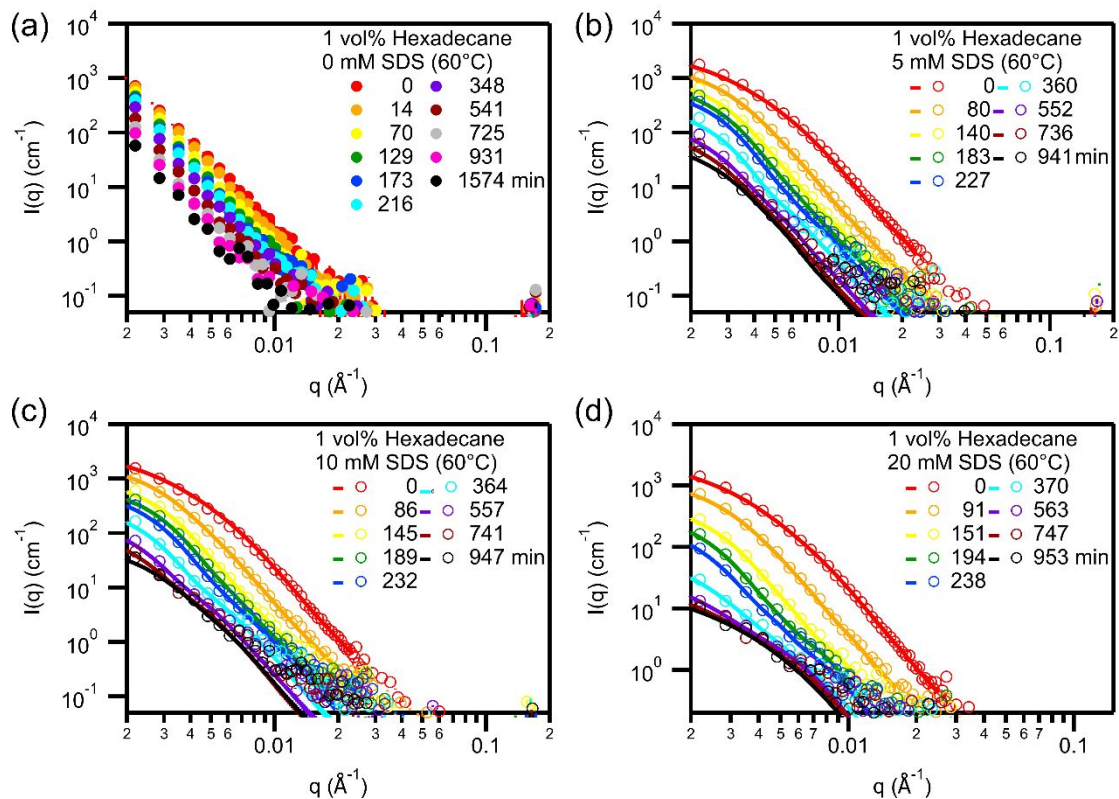


Figure S9. Oil exchange between hexadecane droplets with the presence of (a) 0, (b) 5, (c) 10, and (d) 20 mM SDS (60 °C). Lines represent fits to a polydisperse sphere model (Eq. 1 and 2 in manuscript).

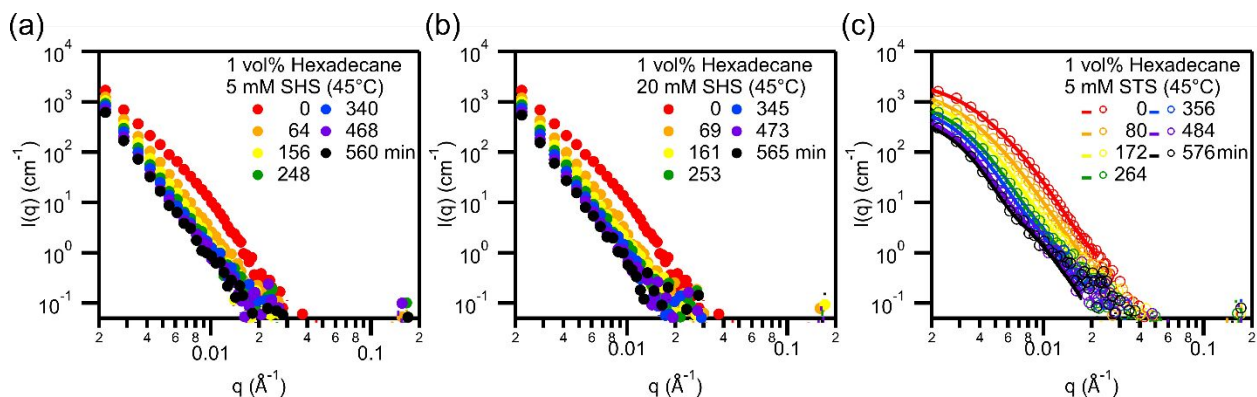


Figure S10. Oil exchange between hexadecane droplets with the presence of (a) 5 mM SHS, (b) 20 mM SHS, and (c) 5 mM STS at 45 °C. Lines represent fits to a polydisperse sphere model (Eq. 1 and 2 in manuscript).

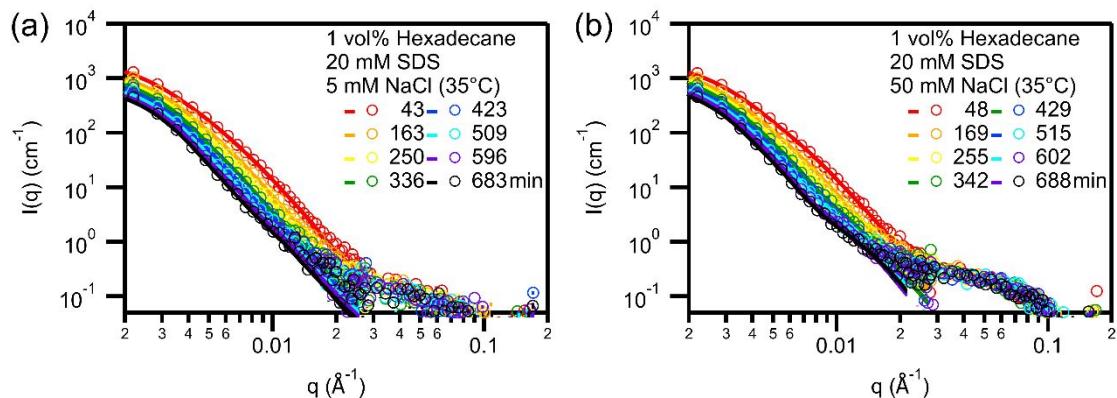


Figure S11. Oil exchange between hexadecane droplets stabilized by 20 mM SDS in (a) 5 mM and (b) 50 mM NaCl at 35 °C. Lines represent fits to a polydisperse sphere model (Eq. 1 and 2 in manuscript).

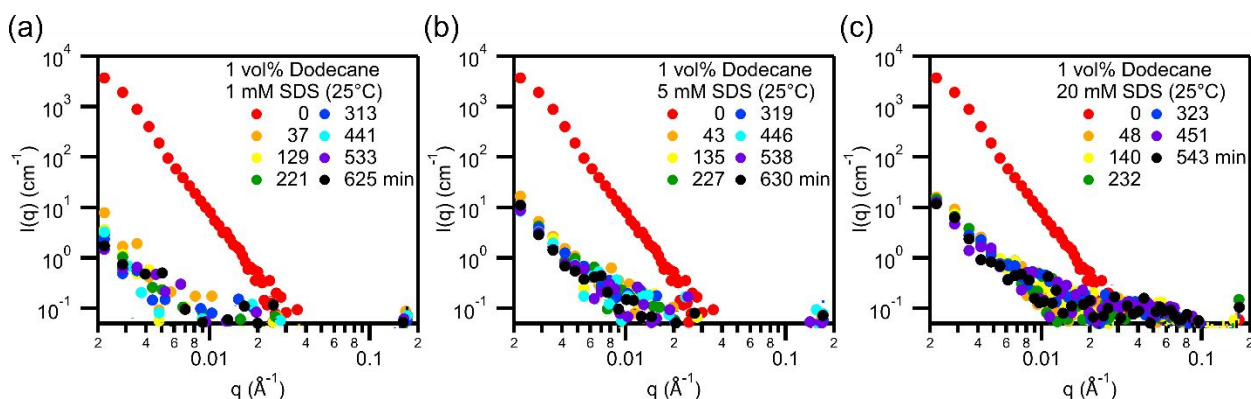


Figure S12. Oil exchange between dodecane droplets stabilized by (a) 1 mM, (b) 5 mM, and (c) 20 mM SDS at 25 °C.

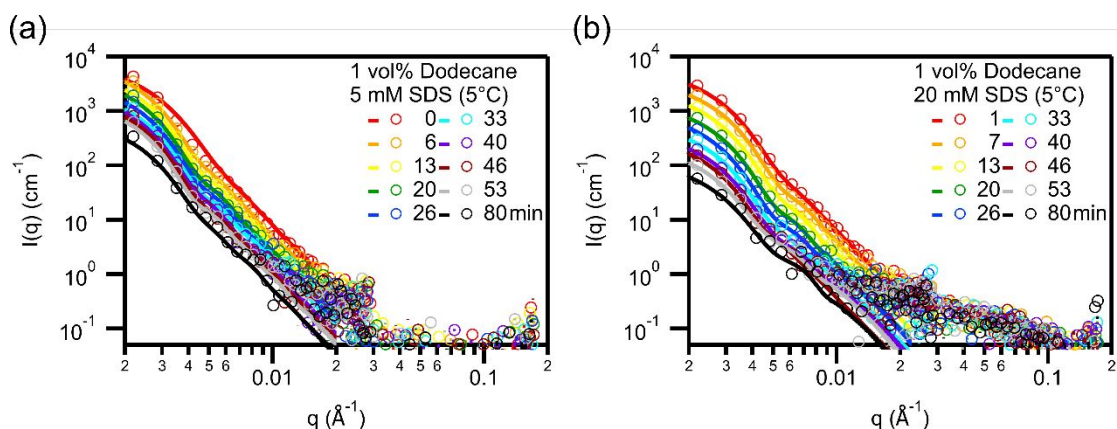


Figure S13. Oil exchange between dodecane droplets stabilized in (a) 5 mM and (b) 20 mM SDS at 5 °C. Lines represent fits to a polydisperse sphere model (Eq. 1 and 2 in manuscript).

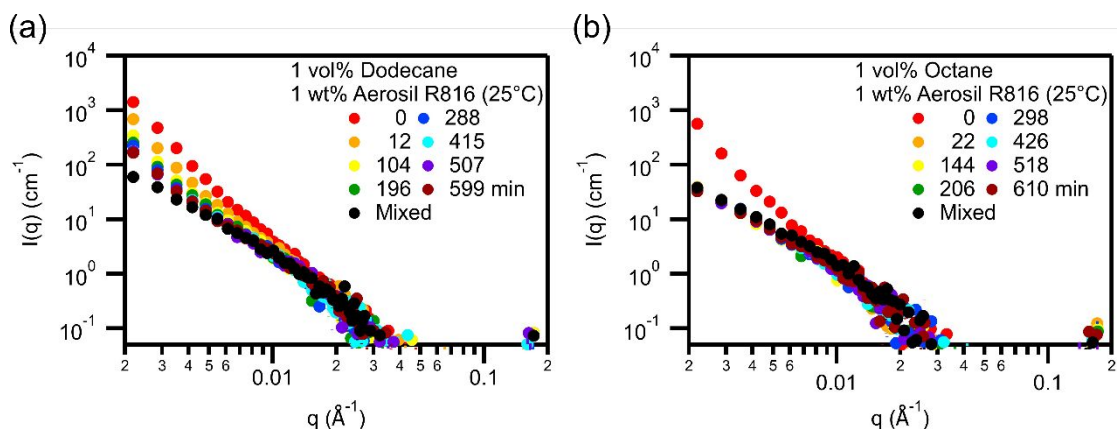


Figure S14. Oil exchange between silica particle stabilized Pickering emulsions with (a) dodecane and (b) octane as the emulsion core at 25 °C.

Explanation on using the normalized contrast vs relaxation function

A more direct method of analyzing the oil exchange kinetics is to estimate the normalized system contrast using the ‘scale factor’ (volume fraction multiply by the square of contrast) which could be estimated by fitting the recorded scattering profiles with a polydisperse sphere model. One advantage of using this method is that the estimated contrast would not be affected by the droplet size change over time. An example of the estimated decay curve using this method and its comparison with the relaxation function at 60°C, where the droplet size change over time is most prominent, is shown in Figure S15. As can be seen, the estimated decay curve is extremely similar to the one obtained using the relaxation function. The estimated kinetic decay constants and plateau values are summarized in Table S1. However, one main disadvantage of using scale factor to quantify the oil exchange kinetics is that it requires it could only be performed on samples containing smaller sized droplets in which the Guinier region of the scattering profile could be observed. Since the results presented in the manuscript also contain samples with larger droplet sizes, we chose to use the relaxation function to estimate the amount of oil that exchanged. On the other hand, if we could potentially obtain the Guinier regions of the larger droplets we could use this method to directly analyze the oil exchange kinetics.

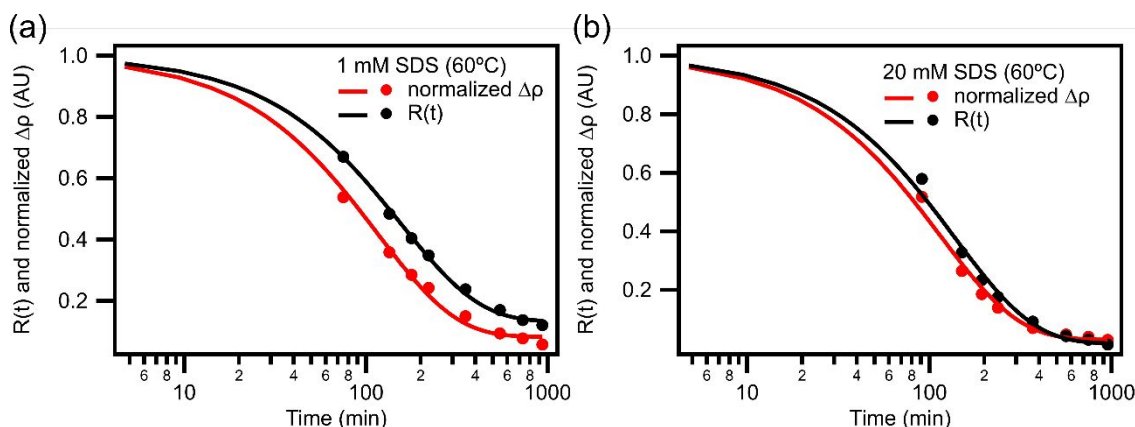


Figure S15. Oil exchange decay curves expressed using a normalized contrast and relaxation function for hexadecane emulsion samples stabilized by (a) 1 and (b) 20 mM SDS at 60 °C.

Table S1. Kinetic decay constants and plateau values estimated using the normalized contrast and relaxation function decay curve.

	1 mM SDS		20 mM SDS	
	k (min ⁻¹)	Plateau (-)	k (min ⁻¹)	Plateau (-)
Normalized contrast method ($\Delta\rho$)	8.64×10^{-3} $\pm 3.61 \times 10^{-4}$	8.23×10^{-2} $\pm 1.06 \times 10^{-2}$	8.74×10^{-3} $\pm 4.39 \times 10^{-4}$	3.01×10^{-2} $\pm 1.29 \times 10^{-2}$
Relaxation function (R(t))	6.42×10^{-3} $\pm 1.57 \times 10^{-4}$	1.33×10^{-1} $\pm 6.78 \times 10^{-3}$	7.24×10^{-3} $\pm 3.60 \times 10^{-4}$	1.70×10^{-1} $\pm 1.45 \times 10^{-3}$

Estimated decay constants for hexadecane emulsions stabilized by SDS at various temperatures

Table S2. Estimated decay constants for SDS stabilized hexadecane emulsion systems.

SDS concentration (mM)	Decay constants k (min ⁻¹)			
	25°C	35°C	45°C	60°C
0	4.90×10^{-4} $\pm 3.16 \times 10^{-6}$	7.59×10^{-4} $\pm 3.00 \times 10^{-5}$	8.40×10^{-4} $\pm 2.54 \times 10^{-5}$	1.43×10^{-3} $\pm 4.41 \times 10^{-5}$
1	9.83×10^{-4} $\pm 1.48 \times 10^{-5}$	1.32×10^{-3} $\pm 5.21 \times 10^{-5}$	2.09×10^{-3} $\pm 7.35 \times 10^{-5}$	6.35×10^{-3} $\pm 1.40 \times 10^{-4}$
2.5	7.71×10^{-4} $\pm 1.28 \times 10^{-5}$	-	-	-
5	7.55×10^{-4} $\pm 8.20 \times 10^{-6}$	1.18×10^{-3} $\pm 4.93 \times 10^{-5}$	2.02×10^{-3} $\pm 6.82 \times 10^{-5}$	5.80×10^{-3} $\pm 1.63 \times 10^{-4}$
10	6.62×10^{-4} $\pm 7.18 \times 10^{-6}$	1.07×10^{-3} $\pm 4.04 \times 10^{-5}$	1.97×10^{-3} $\pm 5.39 \times 10^{-5}$	5.63×10^{-3} $\pm 1.28 \times 10^{-4}$
15	6.33×10^{-4} $\pm 4.66 \times 10^{-6}$	-	-	-
20	7.69×10^{-4} $\pm 5.70 \times 10^{-6}$	1.26×10^{-3} $\pm 2.23 \times 10^{-5}$	2.83×10^{-3} $\pm 4.23 \times 10^{-5}$	7.36×10^{-3} $\pm 2.77 \times 10^{-4}$

Emulsion size estimation

The hydrodynamic size distribution (volume distribution) of emulsions was obtained using dynamic light scattering (DLS) as shown in Figure S16. On the other hand, the size distribution of smaller emulsions could also be obtained by fitting the scattering data with a polydisperse sphere model using Irena (Figures S17-S22 and S24-S26).¹ For example, the initial and final emulsion size distribution of control samples (e.g. 1 vol% D-hexadecane with 20 mM SDS) was estimated and the size distributions at different time points could be expressed using a box and whisker plot (Figure S17). The box portion of the plot, from bottom to top, represents the 25th percentile, median, and 75th percentile of the distribution. The whisker portion represents the 10% percentile and 90% percentile. Based on the results, it could be observed that the overall distribution does not change significantly over the course of the experiment for this sample.

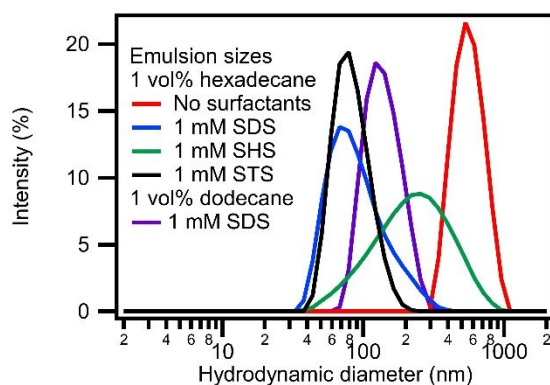


Figure S16. Hydrodynamic size distribution of emulsions obtained using dynamic light scattering.

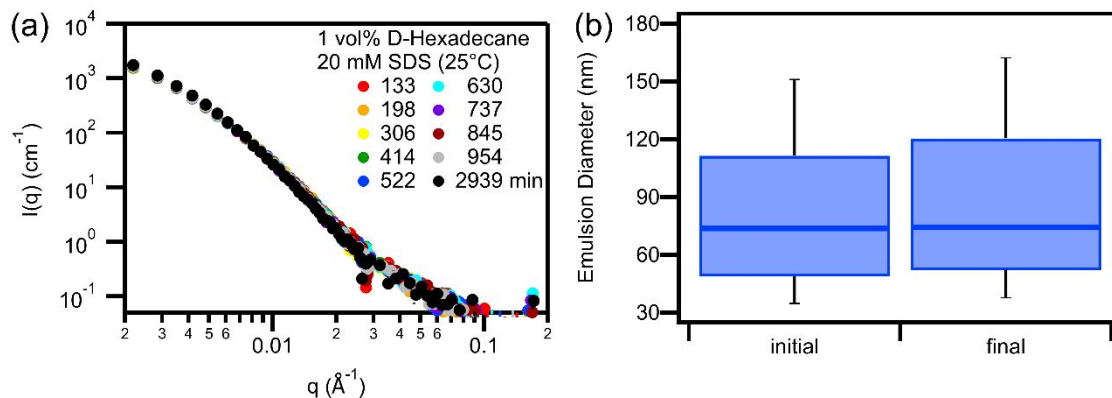


Figure S17. (a) Scattering profile of 1 vol% D-hexadecane with 20 mM SDS tracked over time at 25 °C. (b) Size distribution (box plot) of emulsions at the start and finish of the experiment. The scattering length densities of the emulsion system were $6.67 \times 10^{-6} \text{ \AA}^{-2}$ (D-hexadecane) and $4.54 \times 10^{-6} \text{ \AA}^{-2}$ (solvent)

On the other hand, the scattering profiles and emulsion size distributions does indeed change over time when the samples were at elevated temperature or when stabilized with a lower concentration of surfactants as shown in Figures S18-22. An example scattering profile and its corresponding size distribution is the hexadecane emulsion control sample stabilized with 1 mM of SDS held at 60 °C (Figure S22), which was also the sample that showed the most size change over time.

To account for the variations in size distributions during the time scale of the experiments, additional analysis was performed to estimate their impact on the kinetic analysis. One example of the calculation of the relaxation function with/without accounting for droplet size changes is shown in Figure S23. This sample was chosen because it represented a ‘worst-case scenario’ since it showed the most significant size change in the scattering profile due to the use of lower surfactant concentrations and the sample was held at the highest temperature. Based on the figure, it can be observed that accounting for the changes in droplet size had little effect on the estimated values of the relaxation functions. However, a significant increase in uncertainty was observed at the longer time points due to increasing uncertainty in the control sample’s scattering profiles and the

propagation of error. Fitting the two decay curves resulted in very small changes to the plateau value, from 0.12 to 0.10. On the other hand, the estimated decay constant remained identical ($6.31 \times 10^{-3} \text{ min}^{-1}$). Therefore, the assumption that any changes in droplet size are small over the measured time-scales was used for all of the analysis in this report.

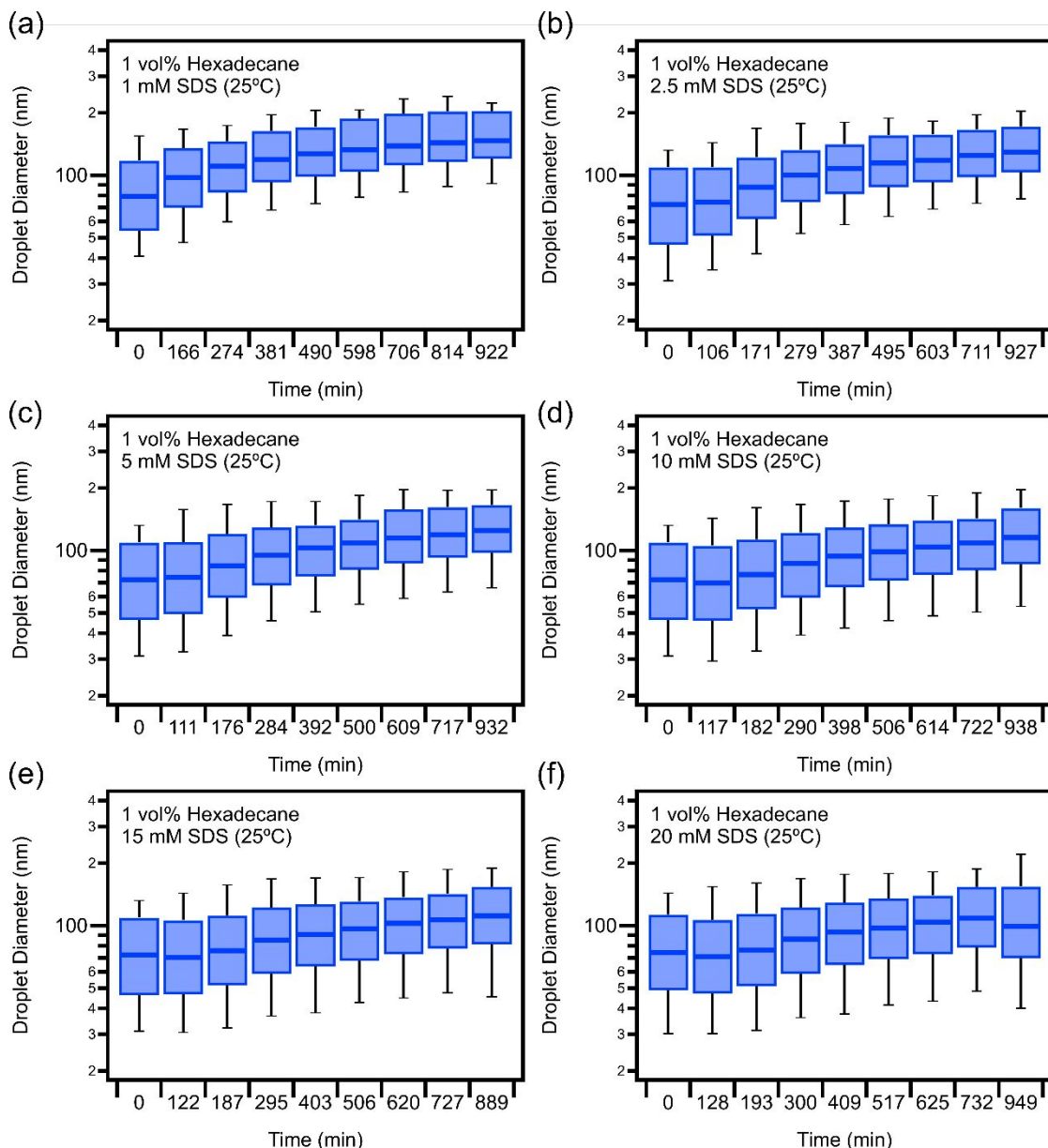


Figure S18. Estimated droplet size from the scattering profiles using a polydisperse sphere model for hexadecane emulsion samples stabilize by (a) 1, (b) 2.5, (c) 5, (d) 10, (e) 15, and (f) 20 mM SDS at 25°C.

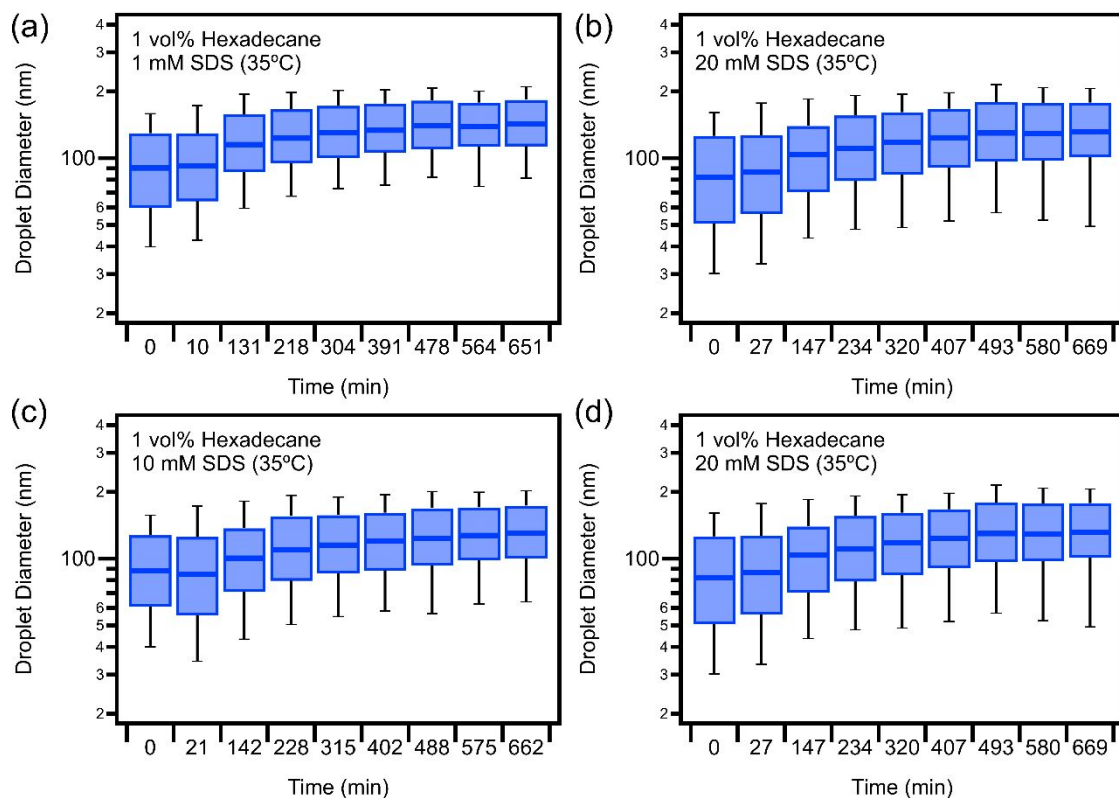


Figure S19. Estimated droplet size from the scattering profiles using a polydisperse sphere model for hexadecane emulsion samples stabilize by (a) 1, (b) 5, (c) 10, and (d) 20 mM SDS at 35°C.

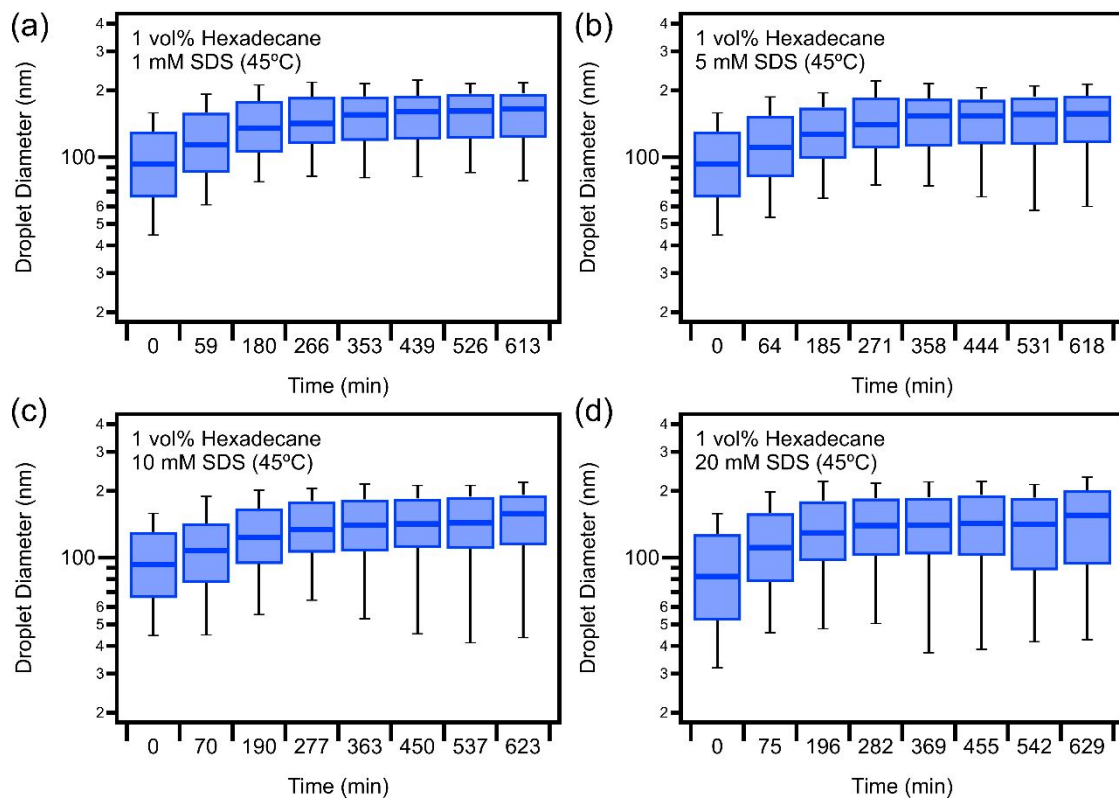


Figure S20. Estimated droplet size from the scattering profiles using a polydisperse sphere model for hexadecane emulsion samples stabilize by (a) 1, (b) 5, (c) 10, and (d) 20 mM SDS at 45°C.

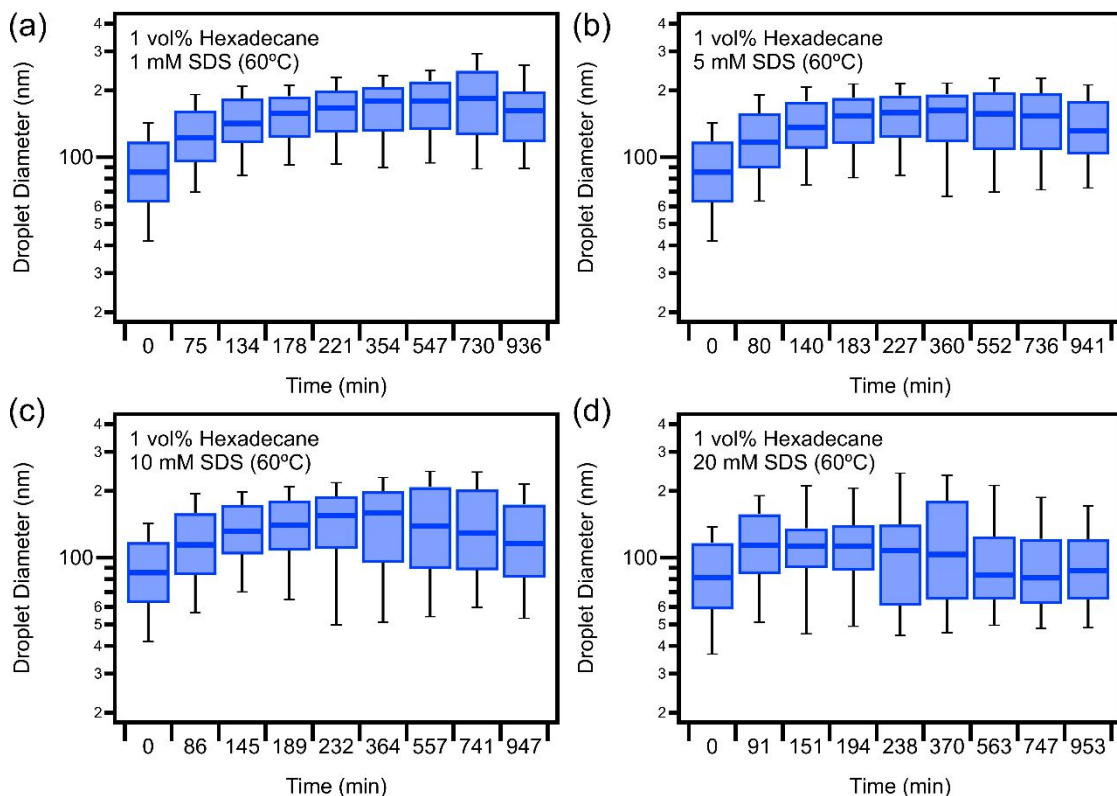


Figure S21. Estimated droplet size from the scattering profiles using a polydisperse sphere model for hexadecane emulsion samples stabilize by (a) 1, (b) 5, (c) 10, and (d) 20 mM SDS at 60°C.

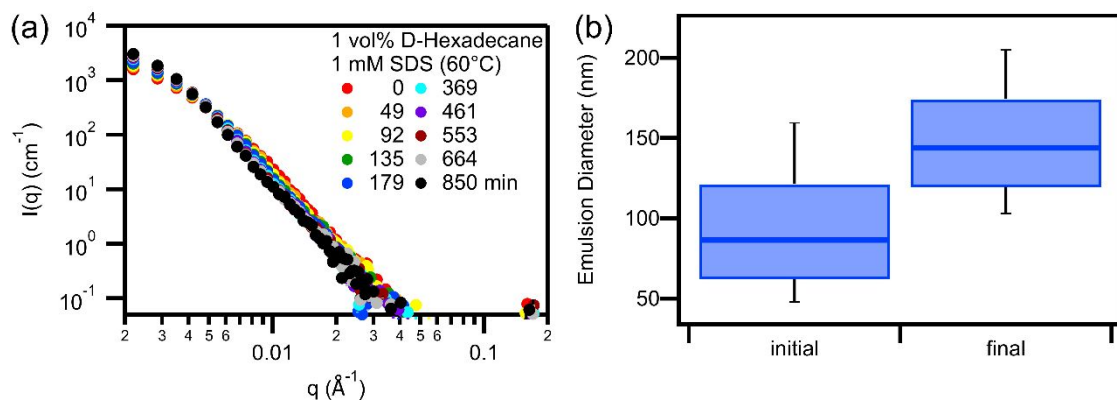


Figure S22. (a) Scattering profile of 1 vol% D-hexadecane with 1 mM SDS tracked over time at 60 °C. (b) Size distribution (box plot) of emulsions at the start and finish of the experiment.

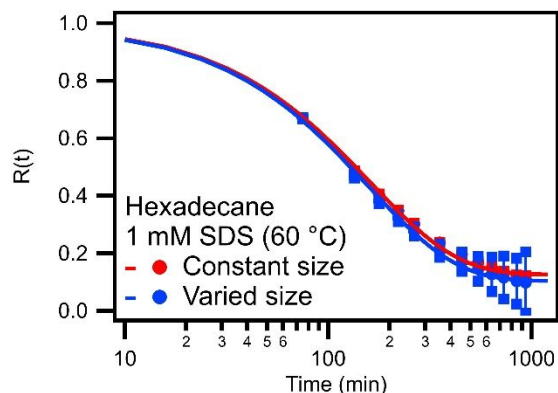


Figure S23. Comparison of the estimated relaxation function for a sample accounting for changes in droplet size versus assuming constant emulsion size. Accounting for emulsion size changes had a minimal effect on the estimated decay constants and plateau values.

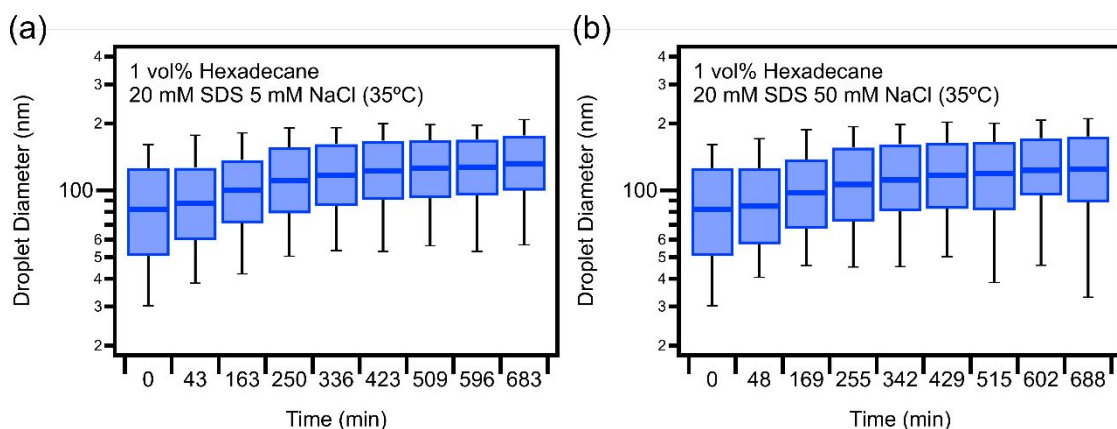


Figure S24. Estimated droplet size from the scattering profiles using a polydisperse sphere model for hexadecane emulsion samples stabilize by 20 mM SDS with (a) 5 and (b) 50 mM NaCl at 35°C.

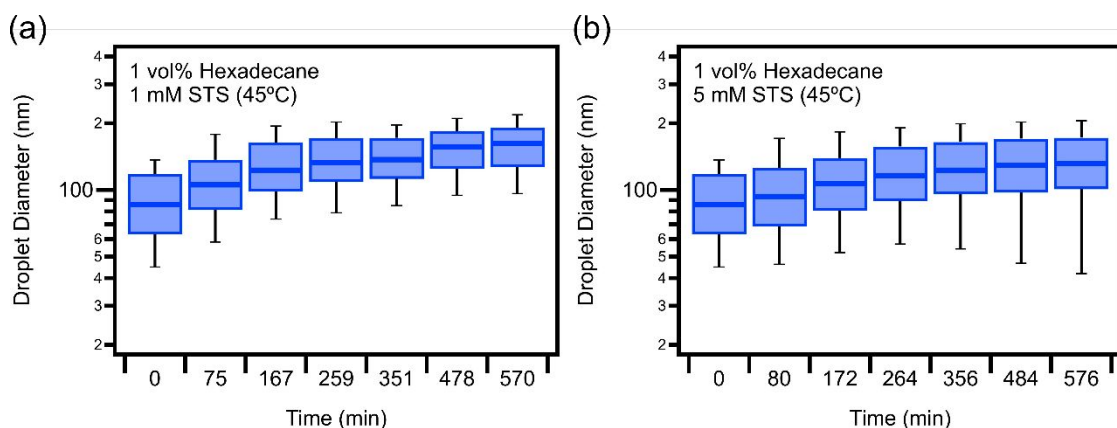


Figure S25. Estimated droplet size from the scattering profiles using a polydisperse sphere model for hexadecane emulsion samples stabilize by (a) 1 and (b) 5 mM STS at 45°C.

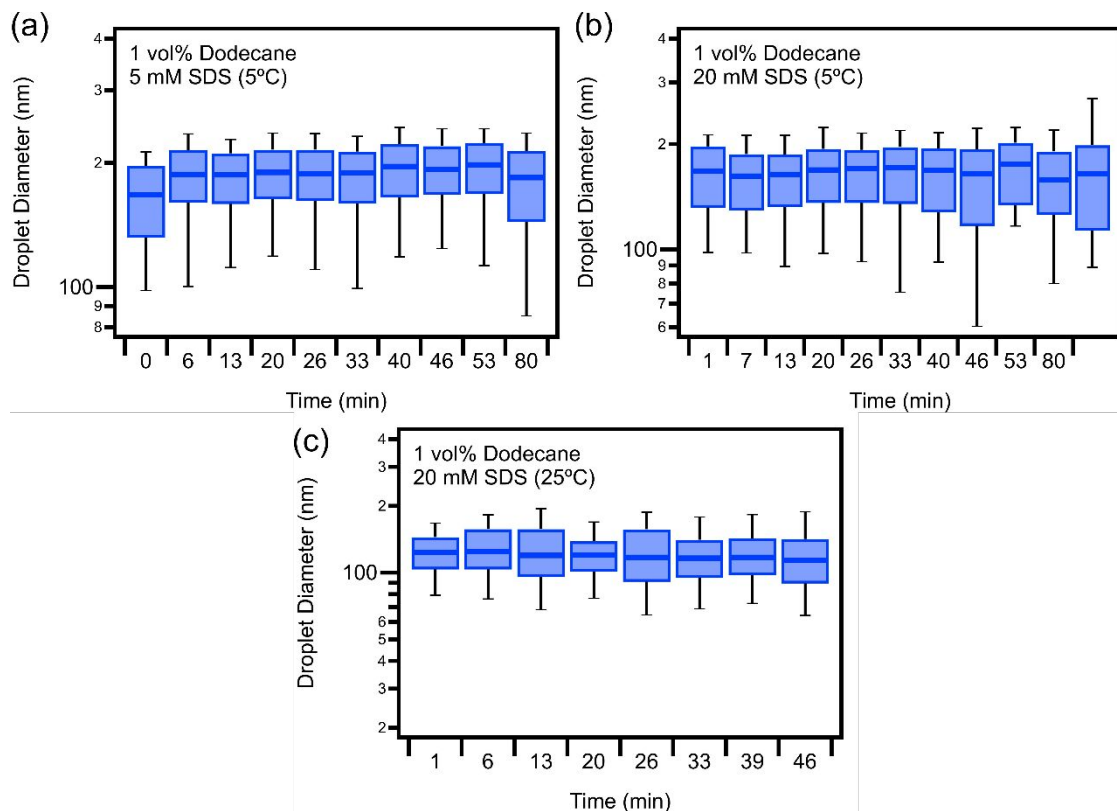


Figure S26. Estimated droplet size from the scattering profiles using a polydisperse sphere model for dodecane emulsion samples stabilize by (a) 5, (b) 20 mM SDS at 5 °C, and (c) 20 mM SDS at 25 °C.

Porod analysis to obtain droplet size

A Porod analysis was performed for larger sized droplets to estimate its mean droplet size. In short, the Porod limit (B) could be obtained by fitting the scattering intensities at the high q region with the Porod function as shown in equation S6. The Porod limit (B) can then be expressed as equation S6 to estimate the specific surface area (S/V), where $\Delta\rho$ is the contrast of the system, S is the total droplet surface area in the sample, and V is the sample total volume.

$$I(q) = \frac{B}{q^4} \quad (\text{S6})$$

$$B = 2\pi(\Delta\rho)^2 \frac{S}{V} \quad (\text{S7})$$

The total sample volume can also be expressed using the average droplet radius (R) and oil volume fraction (Φ_{oil}) and equation S7 can be rearranged to equation S8.

$$R = \frac{3\Phi_{oil}}{\left(\frac{S}{V}\right)} \quad (S8)$$

Estimated droplet sizes using DLS, the Porod analysis, and by fitting the scattering profiles are summarized in Table S3. The diameters estimated from the different analysis method are similar.

Table S3. Mean droplet diameter estimated using DLS, fitting the scattering profiles with a sphere model, and through the Porod analysis.

Emulsions	Mean droplet diameter (nm)		
	DLS (Volume avg.)	Sphere model (Volume avg.)	Porod analysis (Surface avg.)
Hexadecane 0 mM SDS	907.4	-	1028.37
Hexadecane 1 mM SDS	97.7	85.51	93.83
Hexadecane 1 mM SHS	261.6	-	220.39
Hexadecane 1 mM STS	85.3	85.90	93.83
Dodecane 1 mM SDS	142.2	123.34	221.64

Examining the critical micelle concentration with the presence of emulsion droplets

The presence of oil droplets in a system could potentially affect the critical micelle concentration (CMC) of a surfactant. Portions of the surfactants decorates the oil-water interface; therefore, the concentration of surfactants in the dispersed phase would be lower than the dosed concentration. On the other hand, the surfactant micelles have been known to solubilize oil molecules into their hydrophobic cores. This could facilitate the formation of ‘swollen’ micelles at lower surfactant concentrations that could also affect transport. Two experiments were performed to examine whether the surfactant’s CMC was affected by the presence of oil droplets in water.

The first experiment was to use small angle neutron scattering (SANS) to determine whether the presence of dissolved oil molecules would affect the surfactant CMC. Two series of surfactant solutions were synthesized. In one series of samples, there was a layer of oil ‘floating’ on top of the aqueous surfactant solution. These samples were synthesized days before performing the SANS experiments such that the oil molecules were allowed to equilibrate and dissolve into the aqueous surfactant solution. Surfactant solutions without the presence of micelles would scatter similar to a solvent only sample. On the other hand, the scattering profiles would show a significant increase in intensity if surfactant micelles were present. The results are shown in Figure S27 and it can be seen that no significant differences in the CMC were observed between the two series of samples. Both samples, with and without equilibrated oil, showed a similar increase in scattering between 8 and 10 mM SDS. This observation suggest that the presence of dissolved oil molecules will not significantly increase or decrease the CMC of SDS.

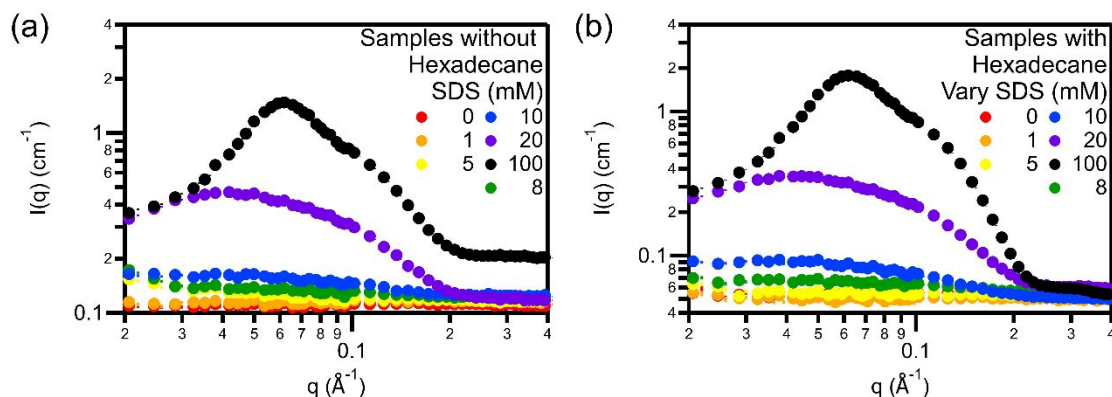


Figure S27. Scattering profiles for (a) SDS solutions and (b) SDS solutions after long-term stabilization (4 days) with an excess layer of hexadecane.

The second experiment was to perform conductivity measurements to obtain the CMC of surfactants in water and in surfactant-stabilized emulsion systems. The CMC of surfactants were first obtained by slowly adding high concentrations of surfactants (e.g. 200 mM SDS) into DI water and monitoring the changes in the sample conductivity (Figure S28 (a), (c), and (e)). A slope

change was observed and the intercept of the two fit lines is the CMC. The measured CMC values for SDS (8.51 mM), STS (1.94 mM), and SHS (299.6 mM) were all close to the theoretically estimated values.

The same experiment was then performed on samples containing 1 volume percent of dispersed hexadecane oil droplets. The estimated CMC for surfactants dissolved in hexadecane emulsions were 11.94 mM for SDS and 5.93 mM for STS. These CMC values are larger than the values obtained from surfactants dissolved in pure water. The increase in CMC is likely due to the adsorption of some surfactant molecules onto the oil-water interface, resulting in a lower effective concentration in the bulk phase. Similar results were also observed by Chang *et al.*² Conductivity measurements for emulsions stabilized by SHS were not performed since the surfactant concentrations used in this study were well below the CMC of the surfactant (~300 mM).

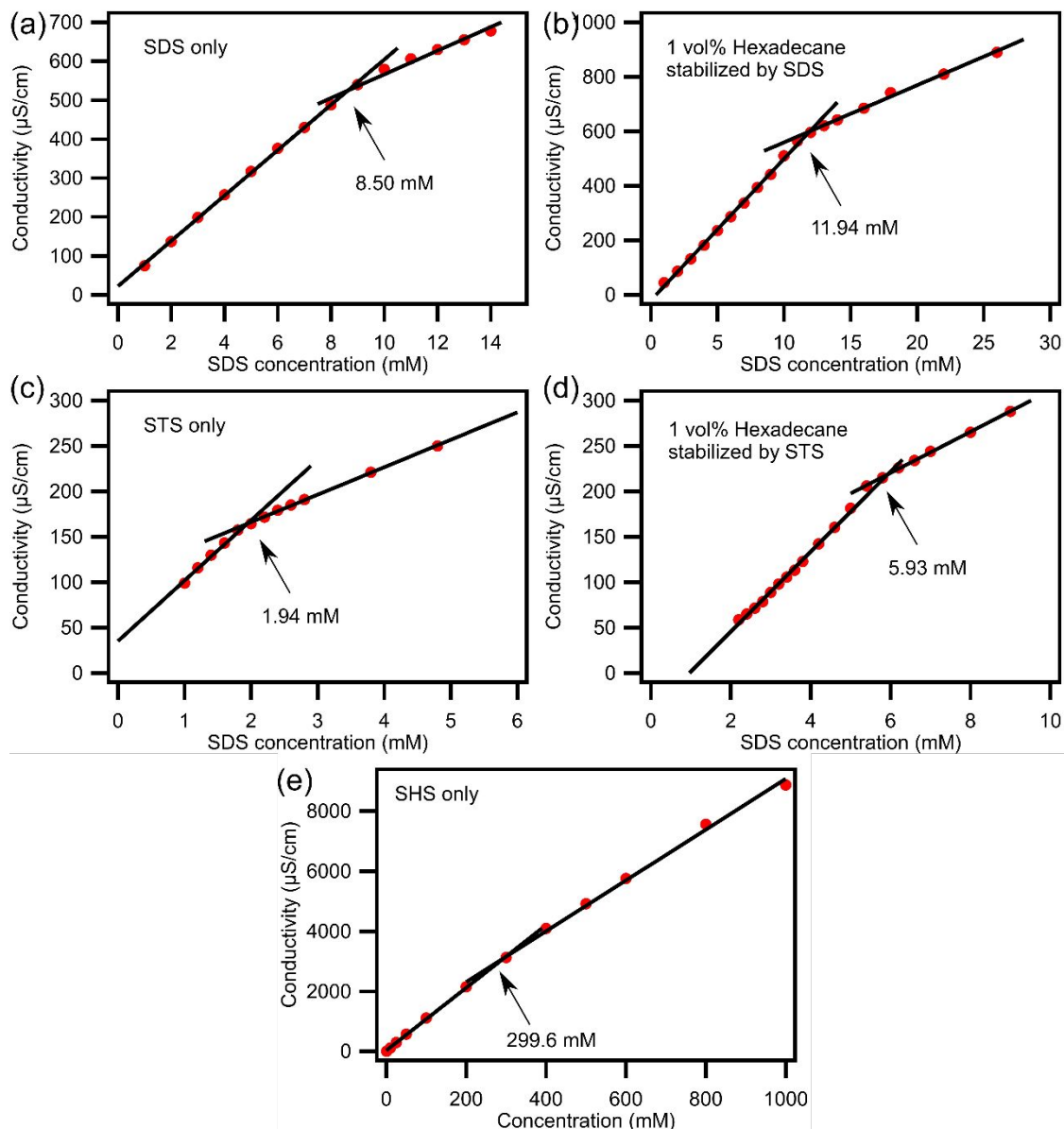


Figure S28. Conductivity measurements of (a) SDS, (b) SDS stabilized emulsions, (c) STS, (d) STS stabilized emulsions, and (e) SHS.

Reproducibility of the experiments

The reproducibility of the oil exchange experiments was examined by comparing the experimental results obtained at two different beamlines, the VSANS and NGB 30 SANS. The relaxation functions estimated using data from the same q range (3.0×10^{-3} to $3.0 \times 10^{-2} \text{ \AA}^{-1}$) of several emulsion systems are almost identical as shown in Figure S29.

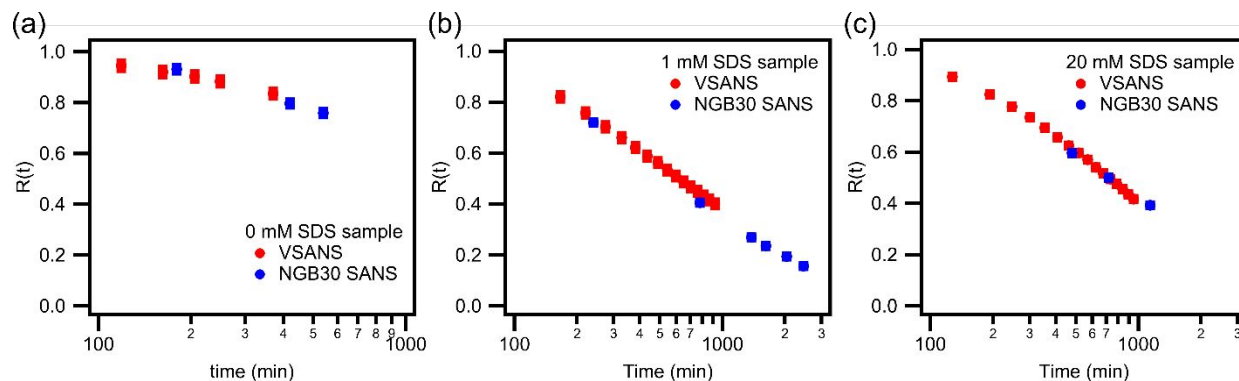


Figure S29. Estimated relaxation function for hexadecane emulsions stabilized by (a) 0, (b) 1, and (c) 20 mM SDS using the VSANS and NGB 30 SANS instrument at National Institute of Standards and Technology Center for Neutron Research.

Scattering profile of sonicating an hexadecane emulsion mixture without the presence of any stabilizing surfactants

The scattering profile 1 vol% hexadecane emulsion sample without the presence of any surfactants sonicated using an in-situ sample environment at NGB30 SANS beamline is shown in Figure S30. Based on the scattering profile, it can be observed that sonication is an effective way of mixing oil materials and synthesizing fully mixed hexadecane emulsion samples where minimal scattering intensities were recorded.

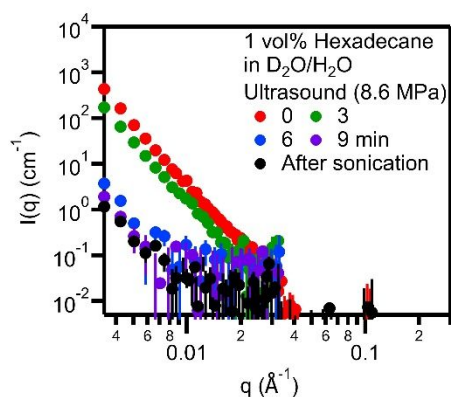


Figure S30. Scattering profiles of sonicating 1 vol% hexadecane using an in-situ ultrasound sample environment (1 cm pathlength) to show that sonication is an effective method for inducing oil exchange between oil droplets.

References:

- (1) Ilavsky, J.; Jemian, P. R. *J. Appl. Crystallogr.* **2009**, *42* (2), 347–353.
- (2) Chang, H.-C.; Lin, Y.-Y.; Chern, C.-S.; Lin, S.-Y. *Langmuir* **1998**, *14* (23), 6632–6638.